Electronic Supplementary Information

High-rate solar-light photoconversion of CO_2 to fuel: controllable transformation from C_1 to C_2 products

Saurav Sorcar[a], Jamie Thompson[b], Yunju Hwang[a], Young Ho Park[a], Tetsuro Majima[c], Craig A. Grimes[d], James R. Durrant[b] and Su-Il In[a,*]

*Email: insuil@dgist.ac.kr

[a]Department of Energy Science & Engineering, DGIST, 333 Techno Jungang-daero, Hyeonpung-myeon, Dalseong-gun, Daegu-42988, Republic of Korea.

[b]Department of Chemistry and Centre for Plastic Electronics, Imperial College London, London SW7 2AZ, UK.

[c]The Institute of Scientific and Industrial Research (SANKEN), Osaka University, Mihogaoka 8-1,
Ibaraki, Osaka-567-0047, Japan

[d]Flux Photon Corporation, 6900 Darcy Lane, Raleigh NC-27606, USA.

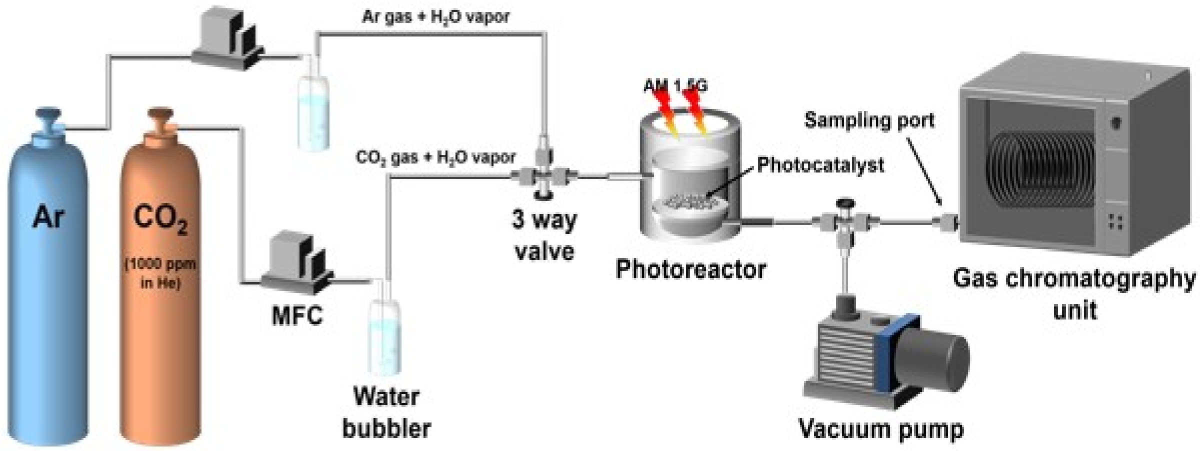

Fig. S1: Depiction of experimental setup used for photocatalytic CO_2 reduction experiments, including online gas chromatography system for dynamic analysis of gaseous products.

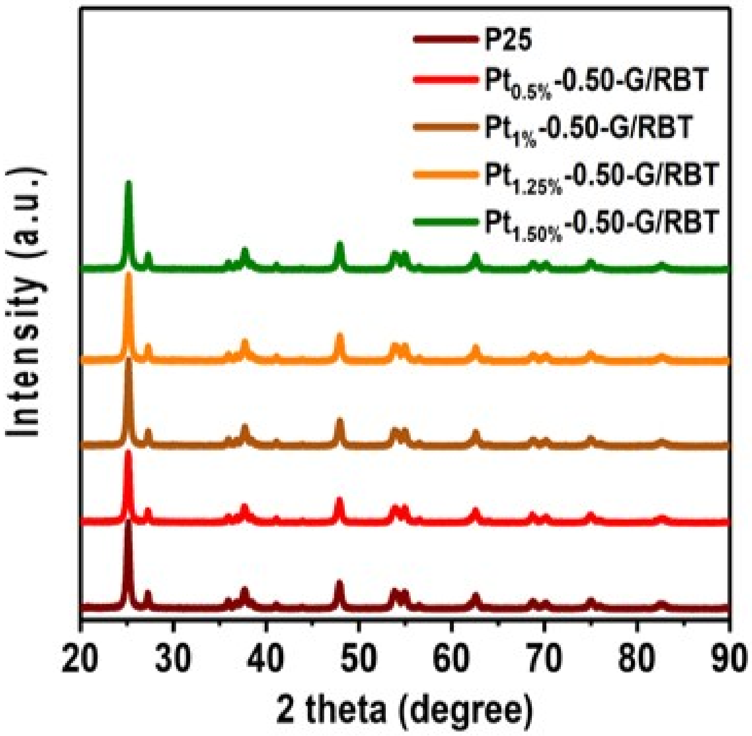

Fig. S2: XRD of Pt sensitized $Pt_{\%}$-0.50-G/RBT samples, where $Pt_{wt\%}$ = 0.50, 1, 1.25 and 1.50 corresponding to theoretically calculated Pt wt. %

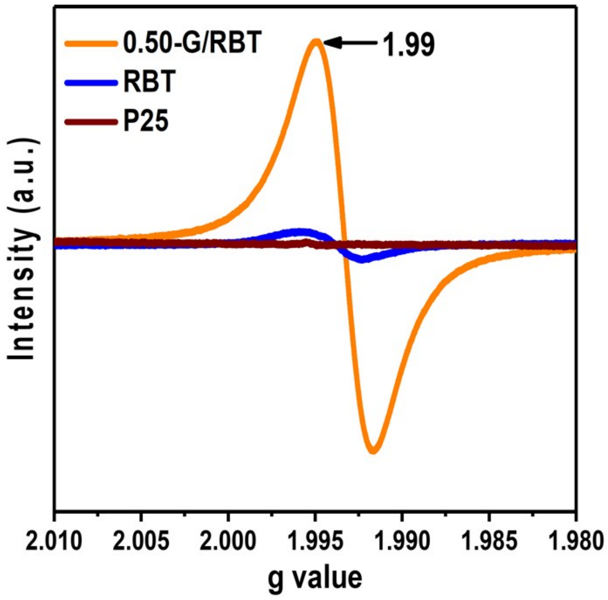

Fig. S3: Electron paramagnetic resonance (EPR) spectra of different samples.

Explanation: The 0.50-G/RBT peak of 1.99 is attributed to the presence of Ti^{3+} states$^{1-3}$. The graphene-wrapping vacuum treatment promotes defects within the TiO_2 and facilitates formation of an intimate junction between Ti of TiO_2 and C present in G (Ti-O-C bonds), as confirmed by HR-TEM, PL, and XPS results.

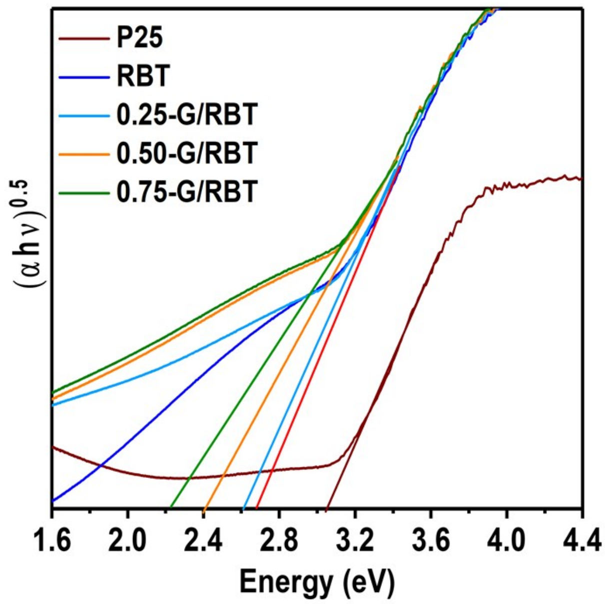

Fig. S4: Band gap determination by Tauc plot analysis.

Table S1. Band gap values obtained from Tauc plot.

Sample	Bandgap (eV)
P25	3.02
RBT	2.68
0.25-G/RBT	2.61
0.50-G/RBT	2.41
0.75-G/RBT	2.22

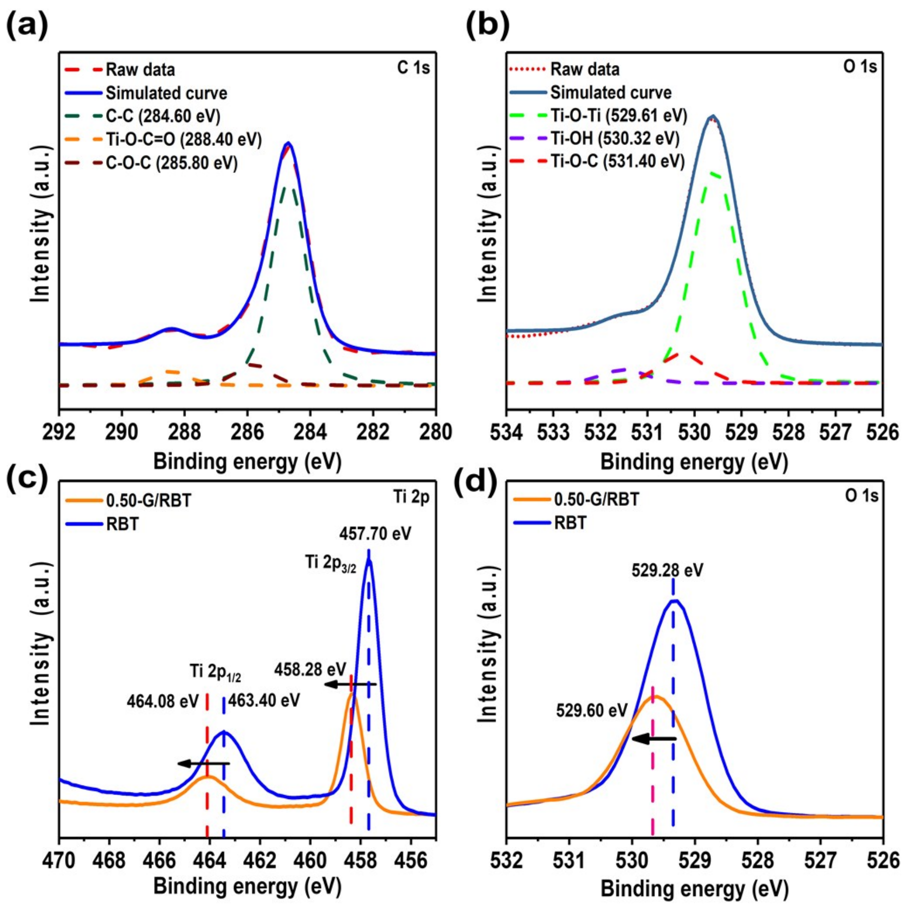

Fig. S5: Core level XPS spectra for representative sample 0.50-G/RBT with regions of: (a) C 1s, (b) O 1s; (c,d) shows the shift in XPS for Ti 2p and O 1s, respectively.

Explanation: XPS was utilized to confirm the interactions between RBT and graphene. **Fig. S5a** shows the C 1s XPS spectra of representative sample 0.50-G/RBT. The strong peak appearing at 284.60 eV is attributed to C-C bonds originating with the sp^2 carbon atoms of graphene[4]. With deconvolution of the C 1s peak, two additional peaks positioned at 285.80 eV and 288.40 eV are observed. The peak at 285.80 eV corresponds to oxygenated carbon species such as C-O-R or O=C-OH[5]. The peak appearing at 288.40 eV is due to Ti-O-C bonds formed by the $Ti(OH)_2$ and carboxyl group of graphene[4]. **Fig. S5b** shows the deconvoluted peaks of O 1s. Three peaks are observed at 529.61 eV, 530.32 eV and 531.40 eV. The first peak at 529.61 eV is mainly due to the Ti-O-Ti bond[6]. Shoulder peaks can be assigned to Ti-OH and Ti-O-C respectively[4,8]. A peak shift was observed for 0.50-G/RBT as compared with RBT, indicating interaction between graphene and RBT[4,7](**Fig. S5c** and **S5d**). The XPS analysis confirms strong interaction between RBT and graphene, achieved by the vacuum annealing.

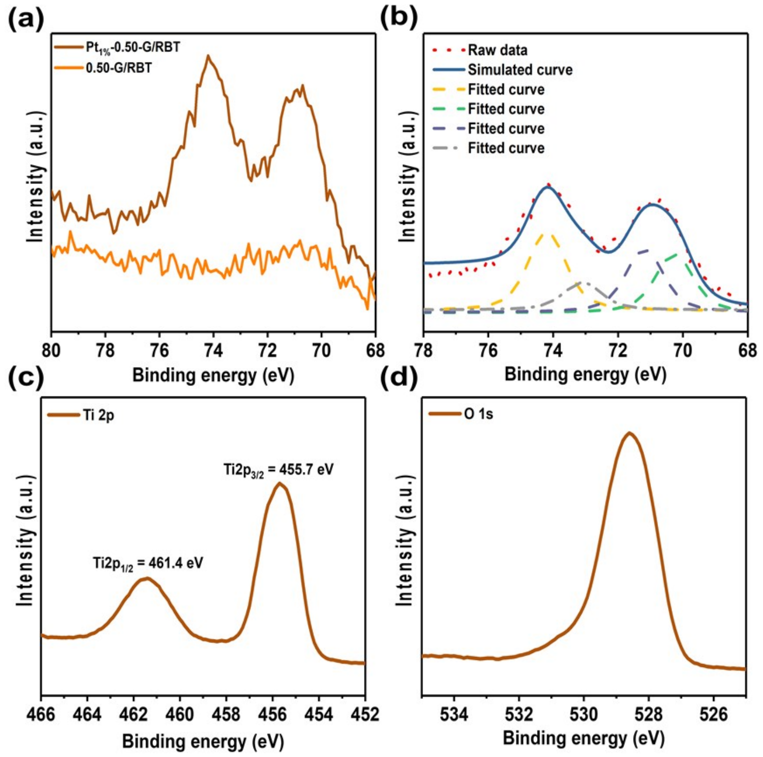

Fig. S6: Core level XPS data of $Pt_{1\%}$-0.50-G/RBT with regions showing: (a) presence of Pt, (b) Pt 4f, (c) Ti 2p, and (d) O 1s.

XPS measurements were conducted for all Pt sensitized samples, see **Fig. S7;** Pt is apparent in all samples.

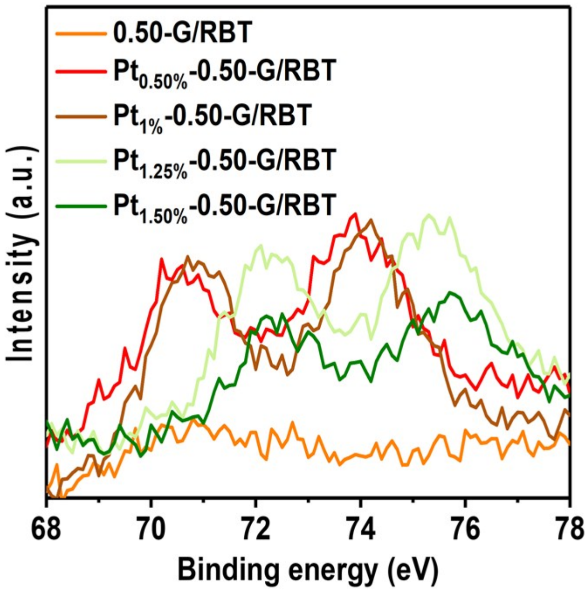

Fig. S7: Pt 4f core level XPS spectra of Pt$_{\%}$-0.50-G/RBT, where Pt$_{wt\%}$ = 0.50, 1, 1.25 and 1.50 corresponding to theoretically calculated Pt wt. %.

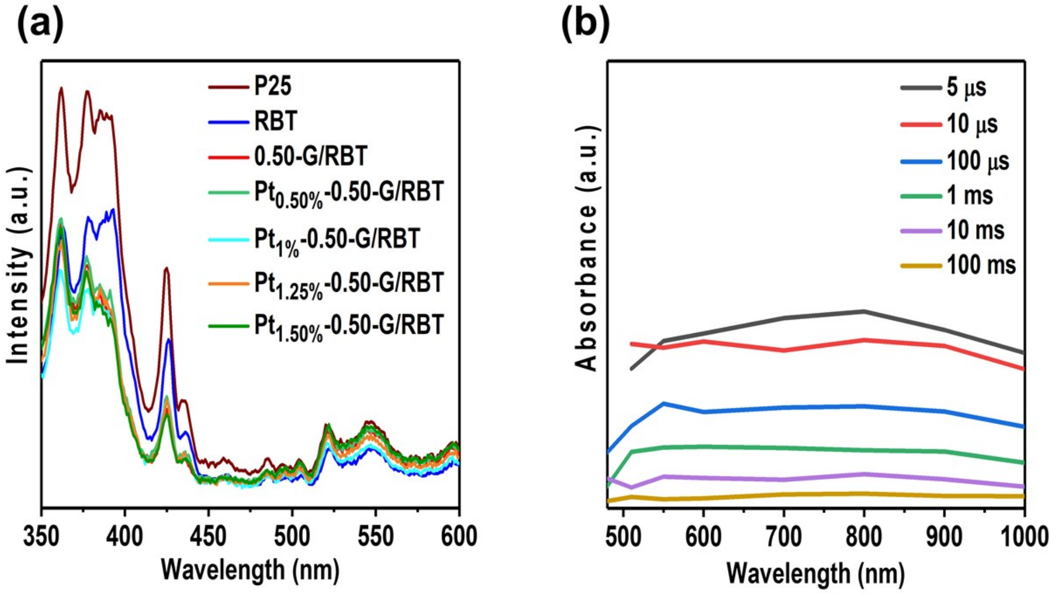

Fig. S8: (a) Photoluminescence spectra of diverse samples, and (b) transient absorption spectroscopy of a $Pt_{1\%}$-0.50-G/RBT sample in which the hole-signature is quenched.

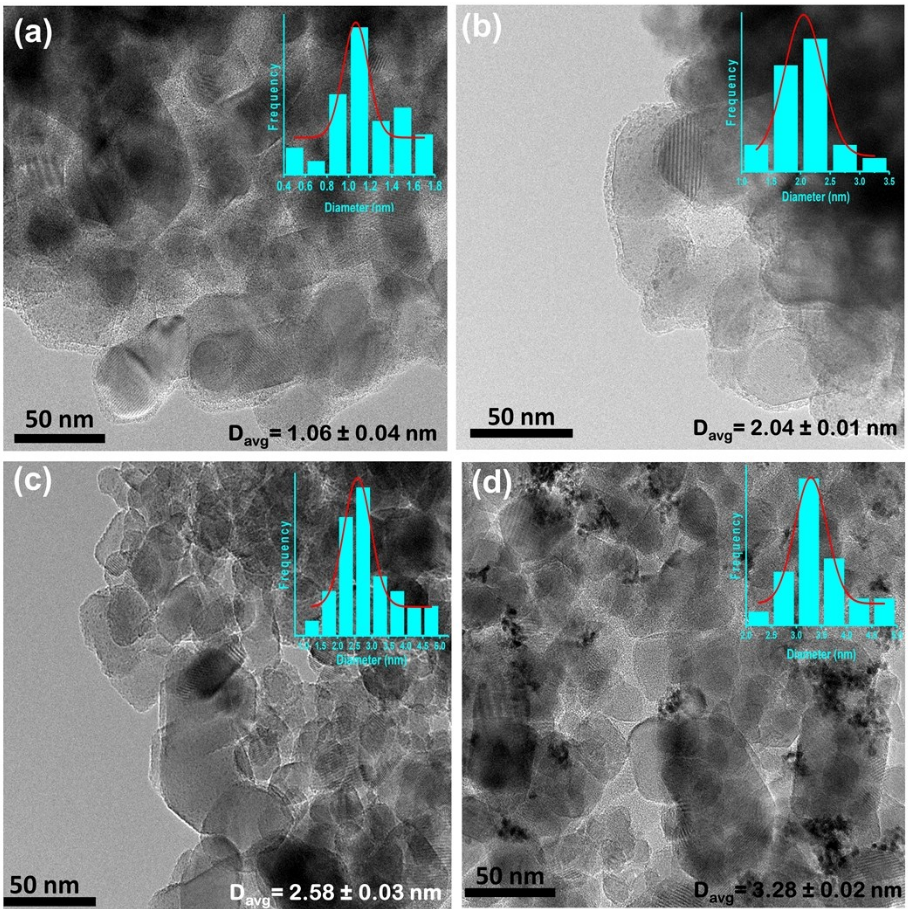

Fig. S9: HR-TEM and Pt particle size distribution of: (a) Pt$_{0.50\%}$-0.50-G/RBT, (b) Pt$_{1\%}$-0.50-G/RBT, (c) Pt$_{1.25\%}$-0.50-G/RBT, and (d) Pt$_{1.50\%}$-0.50-G/RBT.

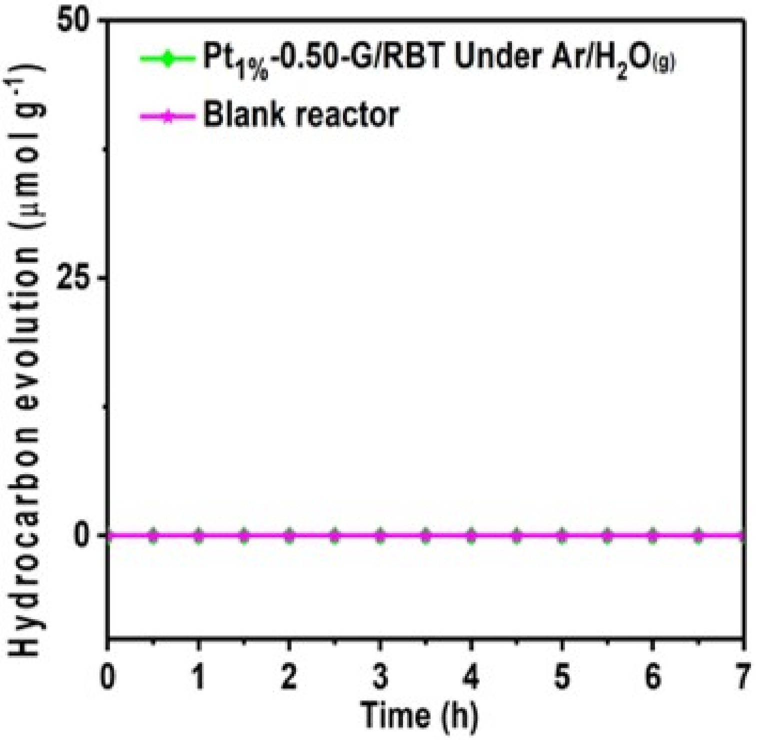

Fig. S10: Photocatalytic control test results for a $Pt_{1\%}$-0.50-G/RBT sample under Ar/H_2O atmosphere, and blank reactor into which CO_2 and water vapour are introduced under AM 1.5G illumination.

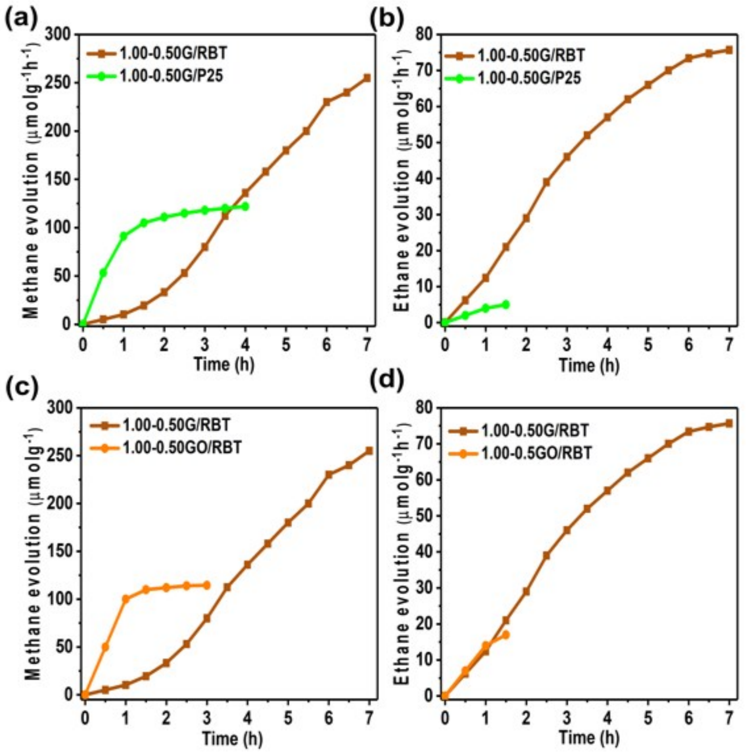

Fig. S11: Cumulative amounts of methane (a,c) and ethane (b,d) by photocatalytic conversion of CO_2 and water vapour over different samples, indicating the effect Ti^{3+} states (a,b) and graphene versus graphene oxide (c,d).

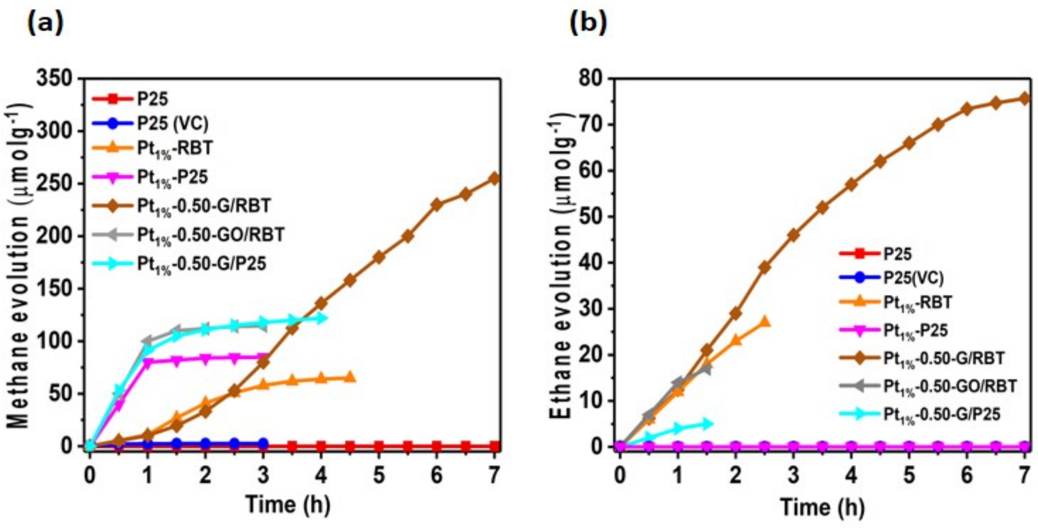

Fig. S12: Cumulative (a) methane, and (b) ethane evolution over different control samples in comparison with Pt$_{1\%}$-0.50-G/RBT.

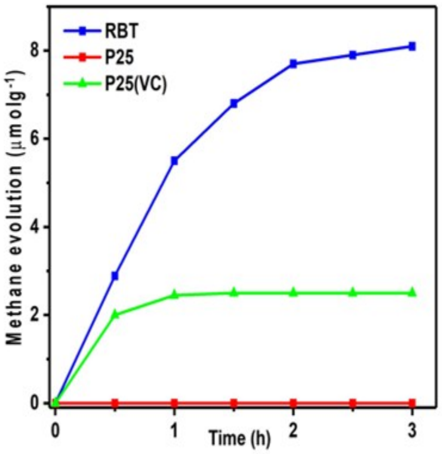

Fig. S13 AM 1.5G photocatalytic activity and stability comparison of reduced blue titania (RBT), P25, and P25(VC) samples.

The results of **Fig. S13** demonstrate P25 nanoparticles, which are only UV active, do not produce any appreciable amount of methane. Sample P25(VC), P25 nanoparticles annealed in a vacuum oven for 90 min at 230 °C produces 2.5 μmolg^{-1} methane. The reduced blue titania (RBT) sample produces 8.1 μmolg^{-1} methane. The RBT sample has superior photocatalytic activity with stable performance up to 3h, while the other two samples are rapidly deactivated. The superior activity of RBT is attributed to its enhanced light absorption and better charge separation, both properties arising from the presence of midgap states[8,9], trivalent titanium ions[1–3], and disordered surface layers[8,10].

Table S2. A comparison of previous works reporting simultaneous evolution of methane and ethane as CO_2 photoreduction products.

Photocatalyst	**Test conditions**	**CH_4 yield**	**C_2H_6 yield**	**Stability**	**AQY (%)**
Au@TiO_2 yolk-shell hollow sphere[11]	300 W Xe arc lamp	Over 10 h, 2.52 µmolg^{-1}h^{-1}	Over 10 h, 1.67 µmolg^{-1}h^{-1}	Not reported	Not reported
Nf/Pd-TiO_2[12]	UV, 300 W Xe arc lamp ($\lambda >$ 300 nm, pH=1)	Over 5 h, ≈1.4 µmolg^{-1}h^{-1}	Over 1 h, ≈0.7 µmolg^{-1}h^{-1}	CH_4 evolution stable for 18 h; C_2H_6 ≈1 h	Not reported
G-TiO_2[13]	300 W Xe arc lamp	Over 4 h, 10.1 µmolg^{-1}h^{-1}	Over 4 h, 16.8 µmolg^{-1}h^{-1}	Not reported	Not reported
Current work	*100 W Solar simulator (AM1.5G)*	*Over 7 h, 37 µmolg^{-}h^{-1}*	*Over 7 h 11 µmolg^{-1}h^{-1}*	*Stable for 42 h*	*7.9 % (5.2 % CH_4, 2.7 % C_2H_6)*

References

1 M. Anpo, M. Che, B. Fubini and E. Garrone, *Top. Catal.*, 1999, **8**, 189–198.

2 S. Zhu, S. Liang, Y. Tong, X. An, J. Long, X. Fu and X. Wang, *Phys. Chem. Chem. Phys.*, 2015, **17**, 9761–9770.

3 K. Sasan, F. Zuo, Y. Wang and P. Feng, *Nanoscale*, 2015, **7**, 13369–13372.

4 T. Lu, R. Zhang, C. Hu, F. Chen, S. Duo and Q. Hu, *Phys. Chem. Chem. Phys.*, 2013, **15**, 12963.

5 L. C. Sim, K. H. Leong, S. Ibrahim and P. Saravanan, *J. Mater. Chem. A*, 2014, **2**, 5315–5322.

6 S. Sorcar, A. Razzaq, H. Tian, C. A. Grimes and S.-I. In, *J. Ind. Eng. Chem.*, 2017, **46**, 2–10.

7 D. Peng, W. Qin, X. Wu, J. wu and Y. Pan, *RSC Adv.*, 2015, **5**, 77138–77146.

8 S. Sorcar, Y. Hwang, C. A. Grimes and S. Il In, *Mater. Today*, 2017, **20**, 507–515.

9 C. Fan, C. Chen, J. Wang, X. Fu, Z. Ren, G. Qian and Z. Wang, *Sci. Rep.*, 2015, **5**, 11712.

10 J. S. Lee, K. H. You and C. B. Park, *Adv. Mater.*, 2012, **24**, 1084–1088.

11 W. Tu, Y. Zhou, H. Li, P. Li and Z. Zou, *Nanoscale*, 2015, **7**, 14232–14236.

12 W. Kim, T. Seok and W. Choi, *Energy Environ. Sci.*, 2012, **5**, 6066.

13 W. Tu, Y. Zhou, Q. Liu, S. Yan, S. Bao, X. Wang, M. Xiao and Z. Zou, *Adv. Funct. Mater.*, 2013, **23**, 1743–1749.